TECHNICAL PAPER

Mechanical Properties and Abrasive Wear Behaviour of Functionally Graded Al-Si12Cu/Al$_2$O$_3$ Metal Matrix Composite

N. Radhika[1]

Abstract Mechanical properties and abrasive wear behaviour of functionally graded Al-Si12Cu/Al$_2$O$_3$ metal matrix composite fabricated under centrifugal casting technique was investigated and compared with unreinforced aluminium alloy. Hollow cylindrical component with dimensions 150 × 150 × 16 mm was produced under the centrifuging speed of 1200 rpm by incorporating 10 wt% Al$_2$O$_3$ particles of size 30–50 μm. The distribution of the Al$_2$O$_3$ reinforcement particles at outer, middle and inner surfaces in matrix was examined through the microstructural analysis. Hardness and tensile strength of the aluminium alloy and functionally graded composite were tested through microhardness tester and universal testing machine respectively. Abrasive wear of aluminium alloy and functionally graded composite was tested through dry abrasion tester for various loads and speeds on outer, middle and inner surfaces of composite specimens. Scanning electron microscopy analysis was carried out on the fractured tensile specimens and worn out specimens. The results revealed that particles were segregated more on the outer periphery and less on the inner periphery. The mechanical properties and the abrasive wear resistance of the functionally graded material were found higher than the unreinforced alloy. The wear rate was found to increase with increase in load, speed and for the distance from the outer periphery of the casting. The worn out surfaces revealed more cutting and ploughing as a result of three body abrasion wear caused by silica sand particles.

1 Introduction

Aluminium metal matrix composites (AMMCs) are the latent materials for mechanical and tribological applications owing to its superior specific strength, improved hardness and high wear resistance [1]. Aluminium 6061/12 wt% Titanium Diboride (TiB$_2$) composite is fabricated and its mechanical properties are evaluated and compared with the unreinforced aluminium alloy. Results reveal that there is significant increase in hardness and tensile strength in the aluminium composite than that of the unreinforced alloy [2]. Aluminium/Alumina (Al$_2$O$_3$) metal matrix composites (MMCs) with different wt% of reinforcement have been fabricated under the stir casting process and its mechanical properties are investigated under the effect of process parameters. It is concluded from the results that hardness increases with the increase in stirring time and wt%, and decreases with increase in reinforcement size [3]. Hybrid aluminium/zircon sand/graphite MMC has been fabricated under the stir casting technique and investigated for its mechanical properties in as-cast and heat treated conditions. The results show that hardness get improved by around 13 % in the heat treated hybrid composite than that of the as-cast composite [4].

Wear behavior of hypereutectic aluminium alloy is assessed at different load, speed and distance under lubricated and un-lubricated conditions. It is observed that silicon particles in the alloy provide greater wear resistance by resisting its detachment from the aluminium alloy. This reduces the three body abrasion wear mechanism at

✉ N. Radhika
n_radhika1@cb.amrita.edu

1 Department of Mechanical Engineering, Amrita School of Engineering, Amrita Vishwa Vidyapeetham, Amrita University, Ettimadai, Coimbatore 641 112, India

lubricated condition and at unlubricated condition, such that severe abrasive mechanism is found to be dominant [5]. Wear behavior of aluminium/silicon carbide (SiC) (10 and 15 wt%) MMC is studied under the influence of applied load, sliding speed and sliding distance using statistical technique. It is interpreted that increasing the wt% of reinforcement increases the wear resistance and it is observed that sliding distance has the major influence on the wear rate followed by the applied load and sliding speed [6]. Sliding wear behaviour of the aluminium/SiC/Boron Carbide (B_4C) hybrid composite is investigated under the load of 20–100 N and sliding velocity of 1–5 m/s at dry sliding condition using pin-on-disc tribometer. The results reveal that addition of B_4C as the secondary reinforcement has considerable effect in increasing the wear resistance of the composite by forming a rich boron oxide layer [7].

A continuous research on the property improvement of the AMMCs has led to the development of special material. An advanced kind of material that arise out of AMMCs, is the functionally graded material (FGM) which performs multi-functionally in behaviour due to gradual variation in its composition and microstructure. This lead to the extensive usage of these materials in the automotive, aerospace, electronics and defense sectors [8, 9]. The incorporation of the reinforcement particles in these FGM has received larger consideration for production of structural components which requires better mechanical and tribological performance [10]. Since the FGMs are non-homogeneous, special processing methods are essential to accomplish the different characteristics in a single part.

Researchers have employed special techniques such as electrophoretic deposition, electromagnetic separation and various methods for fabrication of FGMs [11, 12]. Studies reveal centrifugal casting as one of the inexpensive and easiest processing technique among various techniques for achieving the non-homogeneous properties in FGMs [13]. To raise the impact of FGM in industries, each behaviour of the FGM has to be investigated in detail. Microstructural characteristics of the Aluminium/Aluminium diboride (AlB_2) composite, fabricated through centrifugal casting has been investigated and it is found that AlB_2 reinforcement particles are distributed across the thickness of the casting and also affirmed that AlB_2 are found maximum at the exterior area of the composite [14].

Aluminium/TiB_2 has been fabricated through centrifugal casting method and micro hardness of the material has been tested. Results reveal that hardness of the material increases as the distance increases from inner periphery of the casting towards outer periphery due to occurrence of more TiB_2 at outer periphery [15]. Mechanical properties of Al359/SiC functionally graded composite fabricated through centrifugal casting with different volume fraction of SiC is investigated and reported that tensile and yield

strength of the composite increases with increase in volume fraction of SiC [16].

Functionally graded composites reinforced with SiC particles has also been investigated for its wear behaviour under the control of various process parameters such as applied load, sliding speed and sliding distance. Results reveal that wear rate increases with increasing the applied load and decreases with increasing the speed [17]. Wear and frictional behaviour of spray deposited reinforcement on aluminium functionally graded composite has been investigated and reported that frictional coefficient of FGM decreases when load and speed gets increased. It is also concluded that wear and frictional behaviour depends upon the gradual distribution of the reinforcement particles in composite [18].

From the literature survey, it is observed that there are studies on the characterization of different particle reinforced FGMs but the three body abrasive wear performance of alumina (Al_2O_3) reinforced FGM has not been explored. Therefore, the current study is to deal with the fabrication of functionally graded aluminium metal matrix composite (FGAMMC) reinforced with Al_2O_3 and investigating both mechanical and tribological behaviour for its broad usage in all aspects.

2 Material Selection

The Al-Si12Cu alloy is preferred as the matrix due to its extensive applications in automotive industry, especially in pistons due to its good wear resistance. The reinforcement chosen was Al_2O_3 (10 wt%) with an average size of 30–50 μm. This hard reinforcement was chosen because of good abrasion resistance. The densities of Al-Si12Cu alloy and Al_2O_3 are 2.70 and 3.95 gm/cm^3 respectively. The elemental composition of Al-Si12Cu alloy is shown in Table 1.

3 Experimental Procedure

The stir casting process involves the melting of an alloy in the furnace and addition of the reinforcement particles to the molten metal followed by mechanical stirring. Stir

Table 1 Elemental composition of Al-Si12Cu alloy

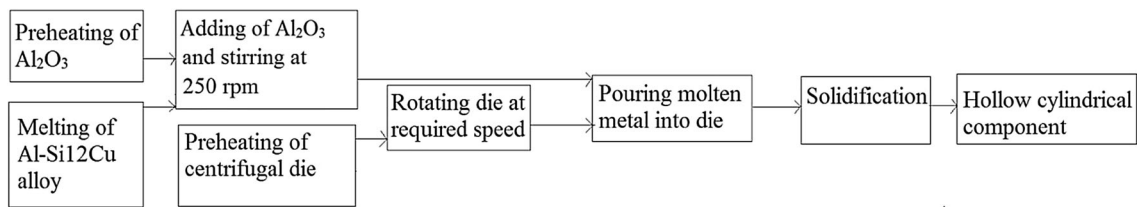| Chemical composition	(%)
Al	83.39
Si	10.9
Fe	0.527
Cu	1.31
Mg	1.05
Ni	2.32
Others (Mn, Cr, Zn, Sn, Ti, Pb, Ca)	0.494

Fig. 1 Schematic illustration of fabrication process of FGAMMC

casting process followed by centrifugal casting is employed for fabrication of functionally graded Al-Si12Cu/Al_2O_3 metal matrix composite. The schematic illustration of the fabrication process is shown in Fig. 1. The aluminium ingots are taken in the graphite crucible for melting in an electric resistance furnace. The melting takes place in an inert gas atmosphere which avoids the unnecessary chemical reactions and reduces the oxidation within the heating chamber to obtain defect free casting. Subsequent to the molten stage of the aluminium alloy, the preheated Al_2O_3 reinforcement particles are added through the hopper provided at the furnace. The reinforcement particles are preheated in order to remove the adsorbed gases, surface impurities and moisture from the surface of the particles for good wettability between the molten metal and the reinforcement particles. The stirrer attached to the furnace helps to mechanically mix the reinforcement particles in the molten metal with varying speed with the aid of motor. The rotation of motor is transmitted to the stainless steel stirrer through bevel gear transmission. The molten metal is stirred at the speed of 250 rpm for good dispersion of reinforcement particles in the molten metal.

A centrifugal casting setup (Fig. 2) consists of a permanent metallic die (150 × 150 mm) used for fabrication of the FGM. The die is enclosed within a preheater which helps to preheat the die to reduce the temperature difference between the inner surface of the die and the molten metal. The centrifugal die is preheated to 350 °C and rotated at the speed of 1200 rpm prior to pouring of molten
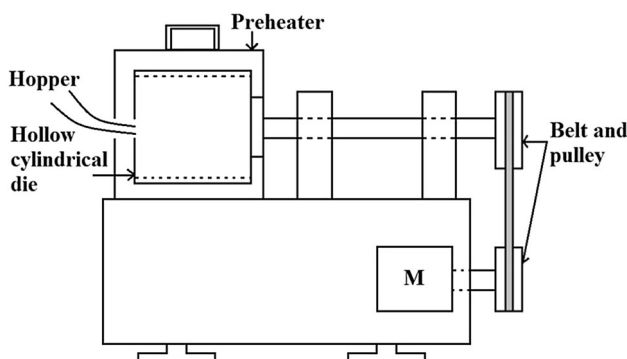
metal. The stirred molten metal is poured at a temperature of 760 °C into the rotating die. The die is made to rotate till the solidification of the molten metal and the solidified part is ejected from the die. The obtained hollow cylindrical component with dimensions of outer diameter 150 mm, length 150 mm and thickness of 16 mm is machined as per the standards for further testing. Al-Si12Cu alloy is also fabricated through conventionally stir casting process for comparison of properties with centrifugally cast functionally graded Al-Si12Cu/Al_2O_3 composite.

4 Microstructural Investigation

The specimens are prepared from the hollow cylindrical cast component to examine the distribution of the Al_2O_3 reinforcement particles resulting from the action of centrifugal force. Three surfaces such as outer, middle and inner surfaces at distance of 1, 7 and 13 mm from the outer periphery are taken for observation since the particles are radially distributed across the thickness of the functionally graded composite. The outer, middle and inner surfaces are metallographically polished for removing the irregularities at the surfaces. The surfaces are primarily polished using belt polisher and then progressively polished using fine emery sheets of grades 1/0 and 2/0 to remove the machining marks. Then, the surfaces are polished with diluted Al_2O_3 in disc polisher to achieve fine surface finish. This surface is finally etched with keller's reagent to examine the microstructure using Zeiss axiovert Inverted metallurgical microscope.

5 Tensile Test

Two different zones such as outer (1–7 mm) and inner (7–13 mm) zone with thickness of 6 mm in the radial direction from the outer periphery of functionally graded composite and specimen from conventionally cast Al-Si12Cu alloy are taken for evaluating the tensile strength using Universal Testing Machine (UTM). The specimens are prepared as per ASTM standard prior to testing. The specimen is fixed in the two jaws and subjected to constant

Fig. 2 Centrifugal casting setup

load by pulling at two ends at the speed of 0.5 mm/min. The specimens (unreinforced aluminium alloy and FGM) obtained after the test are further subjected to fracture surface analysis. This fractural analysis is done using scanning electron microscope (SEM) to understand the influence of reinforcement in the functionally graded composite.

6 Hardness Test

The outer, middle and inner surfaces at distances of 1, 7 and 13 mm in the radial direction from the outer periphery of the casting of the functionally graded composite and specimen from Al-Si12Cu alloy are tested for its micro hardness through Vicker's hardness tester. The specimen is fixed in the specimen holder and load is applied through a diamond indenter for 15 s. The hardness is obtained by measuring the diagonal length of the indentation obtained on the specimen surface. To avoid the error, the hardness is tested at five different places on the same surface and the average value is taken as the hardness value of the surface.

7 Abrasive Wear Test

The three body abrasion test is conducted by means of the dry abrasion tester for various conditions to evaluate the abrasive wear behaviour of the FGAMMC in detail. The specimens of dimensions $75 \times 25 \times 12$ mm are taken from hollow cylindrical component of FGAMMC. The tester is equipped with chlorobutyl rubber wheel to abrade against the specimen which is fixed to the specimen holder. A loading pan is attached to the lever through which the load is applied on the counter face through the specimen. An abrasive medium of silica sand AFS 50/70 is used for producing abrasion on the specimen which is loaded in the hopper and its flow rate is 354 gm/min. This abrasive medium falls between the specimen and the counter face rubber wheel. The test is conducted for different load of 33, 45 and 57 N and varied speed of 75, 125 and 175 rpm on the outer, middle and inner surfaces at distance of 1, 7 and 13 mm respectively from the outer periphery of the casting. The entire tests are conducted for the constant time of 5 min. A similar set of experimental runs are also performed on the Al-Si12Cu alloy for the comparison of abrasive wear performance of the FGM and unreinforced alloy. The specimen is fixed in the specimen holder, required load is applied and test is conducted at the required speed. The specimen is checked for its mass loss by measuring the weight before and after test, and the abrasion wear rate is calculated from the mass loss through the formula

$$W_a = \frac{\Delta G}{dMS} \tag{1}$$

where W_a is the abrasion wear rate (mm^3/Nm), ΔG is mass loss (gm), d is density (gm/mm^3), M is the applied load (N), S is the sliding distance (m).

8 Results and Discussions

The microstructural behaviour, mechanical properties and abrasive wear behaviour are explained in detail in the subsequent sections.

8.1 Microstructural Characteristics

The optical micrographs of the outer, middle and inner surfaces at distance of 1, 7 and 13 mm from the outer periphery of the FGM are shown in Fig. 3a–c. The outer surface at a distance of 1 mm from the outer periphery of the casting reveals maximum reinforcement of particles compared to the middle and inner surfaces at the distance of 7 and 13 mm respectively. This compositional gradient across the thickness of the FGM is mainly affected by the density of the reinforcement and the molten metal. This is also determined by several other factors such as molten metal temperature and mold temperature, applied centrifugal speed (G number), viscosity of the metal, solidification rate and particle size. In centrifugal casting process, the two forces that act on the reinforcement particles are the radial moving velocity—V_c (Eq. 2) and radial buoyancy—F_c (Eq. 3)

$$V_c = \frac{d^2}{18\eta_c}(\rho_p - \rho_l)\omega^2 r \tag{2}$$

$$F_c = \frac{\pi d^3}{6}(\rho_p - \rho_l)\omega^2 r \tag{3}$$

where d—diameter of the reinforcement (m), η_c—the viscosity of the liquid with solid particles (Pa.s), ω—angular velocity of the mold (rad/s), ρ_p and ρ_l—densities of the reinforcement particle and liquid (kg/m^3), and r—distance of the particles from the rotation axis (m). From the above Eq. (2), it is understood that, if $\rho_p < \rho_l$, V_c becomes less than zero and the reinforcement particles moves towards the inner periphery of the casting. As in this case, the density of the Al$_2$O$_3$ reinforcement particles is more than that of the aluminium alloy ($\rho_p > \rho_l$) therefore $V_c > 0$ and hence the reinforcement particles moves towards the outer periphery of the casting [19].

The reinforcement particles segregation at the distance of 1 mm from the outer periphery is mainly due to optimum centrifugal speed and mold temperature. These factors have the control of segregating more reinforcements at
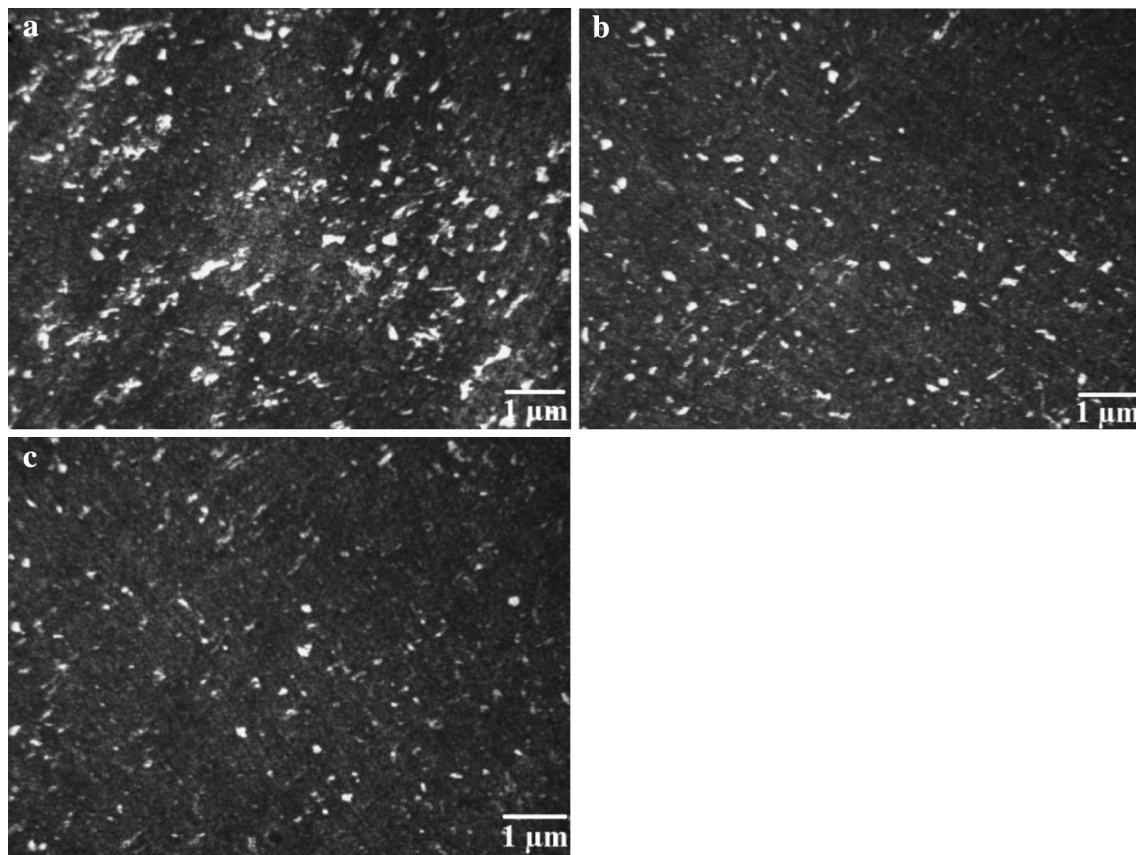
Fig. 3 a–c Optical micrograph of outer, middle and inner surfaces from outer periphery of FGAMMC **a** 1 mm **b** 7 mm and **c** 13 mm

the outer periphery. The centrifugal force and gravitational force acts on the suspended particles in the molten metal during the rotation of the die. The centrifugal force is denoted by $m\omega^2 r$ and the gravitational force is noted as mg. The G number is expressed as the ratio of the centrifugal force to the gravitational force as shown in Eq. (4).

$$G = \omega^2 r/g \qquad (4)$$

ω—mold rotation rate (rad/s), r—radius of the cast cylinder taken (m) and g—acceleration due to gravity (m/s^2). It is understood from the Eq. (4), that the centrifugal force is higher than the gravitational force by G times, hence the gravitational force becomes negligible. It is clear that, as the rotation speed increases, G value increases which eventually increases the reinforcement particle segregation at the outer periphery. The mold is preheated to the temperature of 350 °C to support the segregation of the reinforcement particles by the centrifugal force. The preheat temperature greatly affects the solidification of the cast. The solidification takes place from the outer periphery of the cast and continuous towards inner periphery. The removal of heat from the cast during solidification takes place only through the mold wall. Thus in order to reduce the solidification rate,

the mold is preheated which reduces the temperature gradient between the mold and molten metal. This keeps the molten metal in liquid state for adequate time which allows the reinforcement particle to move to outer periphery of 1 mm. Thus the combined effect of rotating speed of 1200 rpm and mold preheat temperature of 350 °C makes the reinforcement particles to move to the outer periphery of 1 mm.

The middle surface at the distance of 7 mm has reduced level of reinforcement particles which shows that nonlinear distribution occurs across the thickness of the casting. The inner surface at the distance of 13 mm has very less reinforcement particles with large matrix area and forms the particle depleted area. This shows that less dense gas bubbles moves few reinforcement particles along with it towards inner periphery under the influence of centrifugal force [20]. The surfaces at the distances of 1, 7 and 13 mm are observed through the quantitative image analyser and are found to have Al_2O_3 particles concentration as 34, 13 and 8 % respectively.

The fine grain primary aluminium (27 μm) is obtained at the outer surface and the grain size gets coarsened (115 μm) while moving towards the inner periphery. This difference is caused by the dissimilar growth kinetics

during solidification and under the action of centrifugal force. Primarily, the solidification is fast at the mould/metal interface and hence fine grains forms at the outer periphery and coarser grains forms at the inner periphery. The Al_2O_3 reinforcement particles movement towards the outer periphery under centrifugal force during solidification hinders the dendritic growth of aluminium which also contribute to the formation of fine grain structure at the outer periphery. Thus the combined action of fine grain and the particle enriched zone at the outer periphery leads to greater hardness and wear resistance. On moving to the inner periphery, increase in the grain size and decrease in the reinforcement concentration results in decrease in hardness and wear resistance.
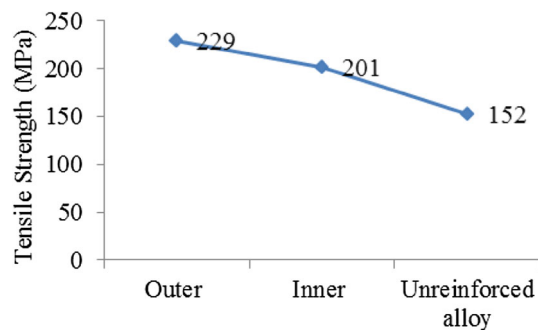

Fig. 4 Tensile strength of Al-Si12Cu alloy and FGAMMC

8.2 Tensile Strength of Unreinforced Alloy and FGAMMC

The obtained tensile strength of the unreinforced Al-Si12Cu alloy and different zones such as outer and inner taken from the FGAMMC is shown in Fig. 4. The outer zone of the FGM shows high tensile strength of 229 MPa due to the existence of more reinforcement particles which has greater bonding with the matrix. Therefore the load acting in the tensile test is transferred from the matrix alloy to the reinforcement particles which act as the load bearing elements which delays the breaking of the specimen.

The inner zone of FGM shows less tensile strength of 201 MPa due to the presence of less amount of reinforcement particles, which cannot resist much pulling force. Therefore the total load acts more on the matrix alloy and thus break the specimen in advance [16]. The unreinforced alloy has lesser tensile strength compared to both the outer and inner zones of the FGAMMC. There is an enhancement of 33 % in tensile strength of the FGM compared to the unreinforced alloy.

The fractural analysis of the broken tensile specimens (Fig. 5) characterizes the failure mode. The local stresses that acts on the composite determines the main fracture mechanisms i.e., reinforcement particles cracking, voids nucleation as a result of interfacial decohesion and fracture
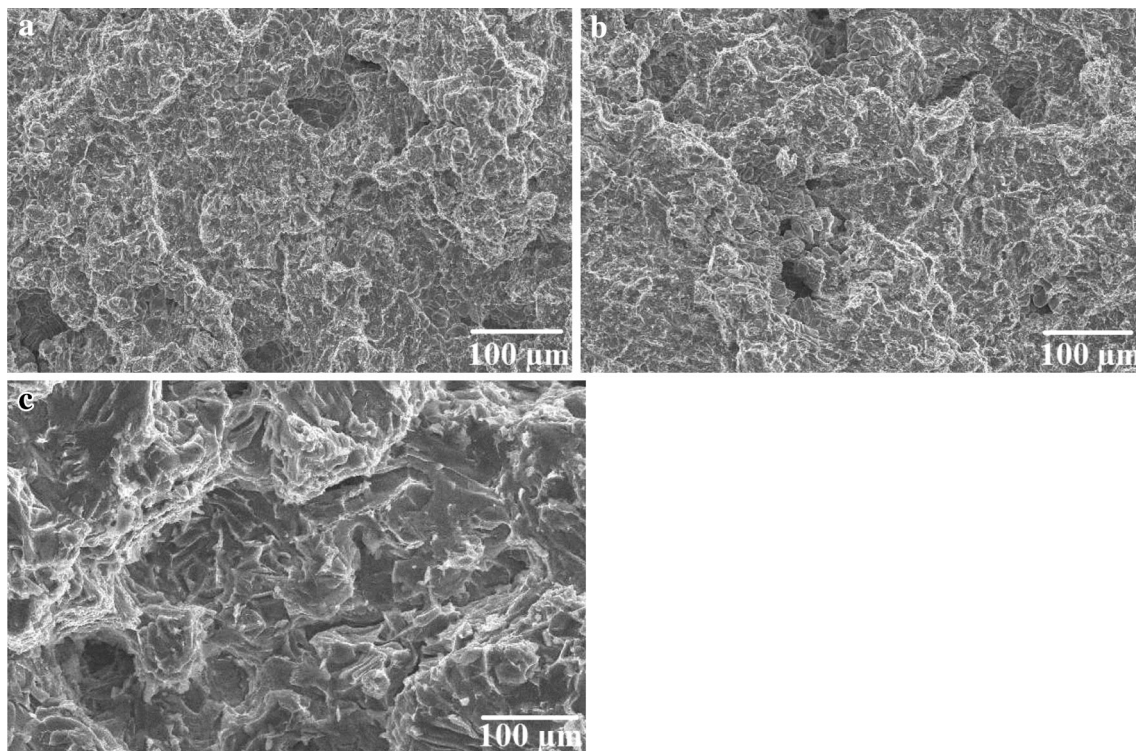

Fig. 5 SEM analysis of fractured tensile specimens **a** Outer zone **b** Inner zone **c** Unreinforced alloy

of the matrix through growth and coalescence of voids. The outer zone (Fig. 5a) which consists of more Al$_2$O$_3$ reinforcement particles shows combined brittle-ductile fracture but dominantly the brittle fracture due to good interfacial bonding of the reinforcement particles with the aluminium matrix. Thus the fracture happens mostly through the reinforcement rather than the interface between the matrix and the reinforcement [21]. The thermal expansion value of the reinforcement particles differ greatly from that of the aluminium alloy and hence it leads to thermal mismatch. This causes the generation of elastic stresses which leads to compression effect on particles and tension effect on the matrix. The concentration of the reinforcement particles is high at this outer zone, hence the fracturing of the particle is greater in this zone. Large particles have less inter-particle distances which provide easy linkage between the cracks/voids in the reinforcement particles. On contrary, the smaller Al$_2$O$_3$ reinforcement particles generally does not tend to crack. In this situation, the action of strain difference between the reinforcement and the matrix causes decohesion of the matrix. Therefore, it is clear that the outer zone of the composite initially fails through fracturing of the reinforcement particles and is progressively followed by the propagation of the crack between the particles through matrix. The inner zone (Fig. 5b) reveals a small number of dimple formations with micro cracking as this is due to the presence of more matrix region with less reinforced region. The unreinforced alloy (Fig. 5c) shows closed packed structure and fails via the normal nucleation of voids and growth in a ductile manner [22].

8.3 Hardness of Unreinforced Alloy and FGAMMC

The hardness enhancement on the outer, middle and inner surfaces at different distances from the outer periphery of the FGM casting and the Al-Si12Cu alloy is shown in Fig. 6. The outer surface at a distance of 1 mm from the outer periphery of the casting shows higher hardness when compared to the middle and inner surfaces at the distance of 7 mm and 13 mm from the outer
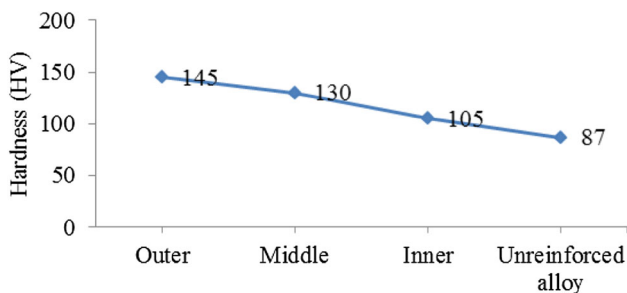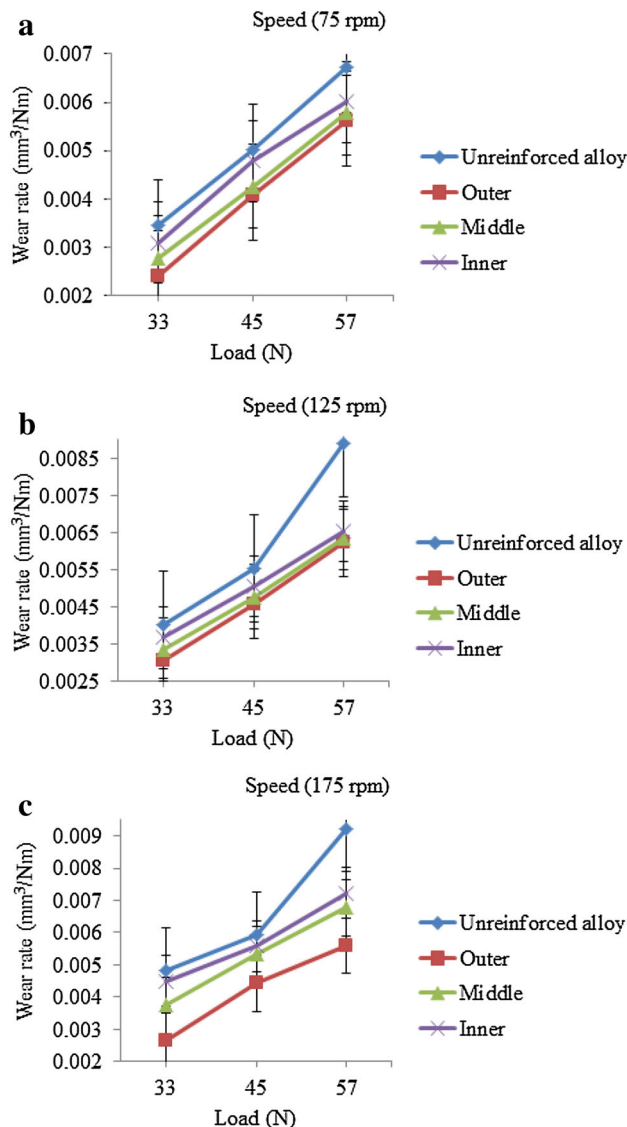

Fig. 7 a–c Effect of load on wear rate

periphery of the casting. This is owing to the segregation of the reinforcement particles towards the outer periphery of the FGM under the centrifugal action. The reinforcement particles have the higher hardness than the matrix alloy which significantly improves the hardness of the surface where it is present in more amount. This surface resists the plastic deformation caused by the indenter and results in less indentation [23]. The greater hardness at the outer periphery is attributed to the Orowan strengthening mechanism as it is dominant in the particle reinforced composites. The Al$_2$O$_3$ reinforcement particles hinder the dislocation motion near to it by acting as the obstacles. The bending of the dislocation takes place between the Al$_2$O$_3$ reinforcement particles which forms loop around the reinforcement particles and leaves forward. The consecutive dislocation forms loop

Fig. 6 Hardness of Al-Si12Cu alloy and FGAMMC

continuously over the particles which induces a back stress that inhibits further movement of the dislocation. Hence greater stress is required for the additional slip process which results in greater strength of the material. The required stress to overcome the back stress is inversely proportional to the distance between the particles. Hence, the particle enriched outer surface of 1 mm has the less inter-particle spacing and exhibits greater hardness.

The surface at distance of 7 and 13 mm has less hardness of 130 and 105 HV respectively compared to 1 mm (145 HV) distanced surface from outer periphery. The middle and inner surfaces have lesser amount of reinforcement particles which is confirmed through the microstructural analysis (Fig. 3b, c) and therefore it is observed that reinforcement particles contribute much towards the hardness of the FGM [24]. The particle depleted inner periphery (13 mm) has high interparticle distance and hence orowan strengthening is not predominant. Thus, less stress is required to deform the material which results in easy deformation of the surface and results in less hardness.

The unreinforced alloy has the least hardness of 87 HV which again shows the influence of the reinforcement particles for the improvement of hardness. Thus it is observed that, hardness in FGM raises to 40 % compared to the unreinforced alloy.

8.4 Abrasion Wear Behaviour

The experimental results obtained through the dry abrasion tests are used for studying the influence of load, speed and distance from the outer periphery of the casting on the abrasion wear rate individually.

8.4.1 Effect of Load on Abrasion Wear Rate

The load is varied in equal intervals of 33, 45 and 57 N on outer, middle and inner surfaces of the FGM respectively which are at a distance of 1, 7 and 13 mm from the outer periphery of the casting and also on Al-Si12Cu alloy. The tests are conducted for the various speeds of 75, 125 and 175 rpm individually and shown in Fig. 7a–c. The abrasion wear rate for the varied load of 33, 45 and 57 N at constant speed of 75 rpm is shown in Fig. 7a. The load has an increasing trend of wear rate on the outer, middle and inner surfaces of the FGM and also on the alloy. This mechanism is observed due to the temperature increase on the surface as the load is increased. It is observed from the plot that the wear values are smaller at lower loads and after the critical load the wear rates are found to be maximum. The wear is indicated by the liberation of vibration at high load condition. The abrasion is caused on the surface by the movement of silica sand medium which falls between the specimen and the rubber wheel.
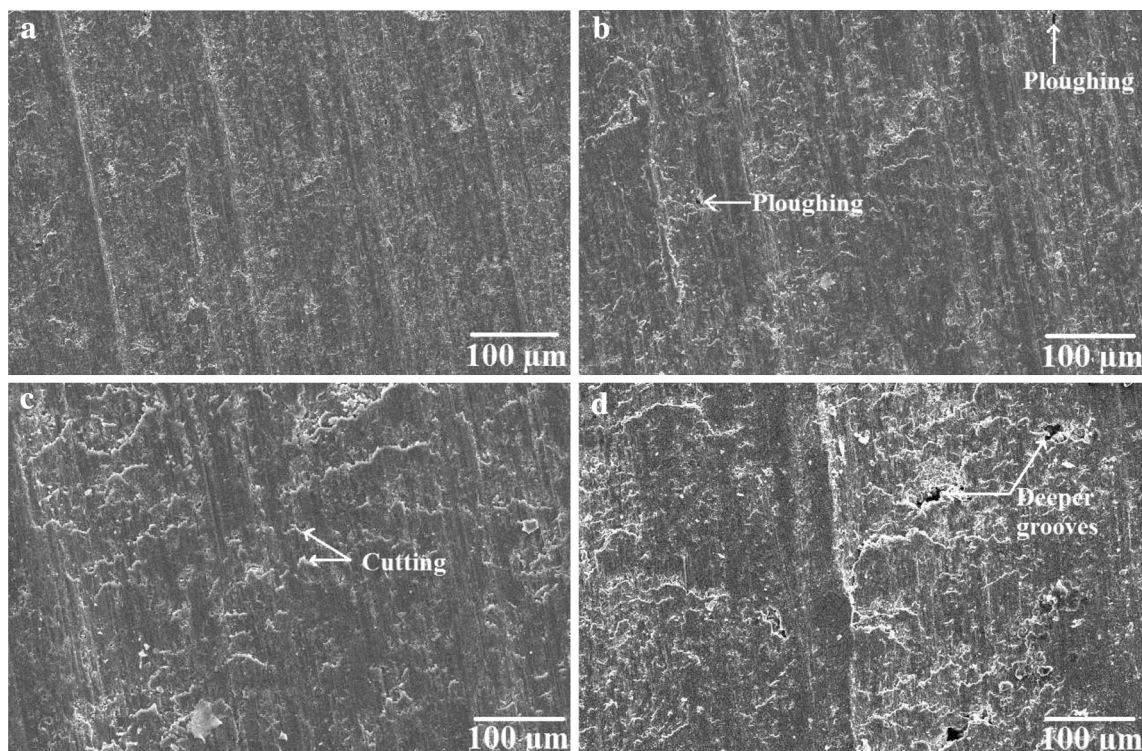

Fig. 8 SEM analysis of outer surface of FGM at **a** 33 N **b** 45 N **c** 57 N and **d** Unreinforced alloy (57 N)

At low loads, the ploughing action of the abrasive medium will be less and result in less wear rate. The increase of the load impress the silica sand much onto to the rubber wheel which inturn makes the sliding abrasive medium to produce more cutting and ploughing action on the specimen surface which results in maximum wear rate [25]. The outer, middle and inner surfaces of the FGM and the unreinforced alloy surface tested by varying the load and at constant speed of 125 and 175 rpm are shown in Fig. 7b, c. The outer surface at the distance of 1 mm also experiences the same trend in wear rate as the load increases on it but shows lower order of wear rates when compared to the surfaces at a distance of 7 and 13 mm respectively. The surface of the unreinforced alloy has the higher wear rate values when compared to all surfaces of FGM and the same behaviour is observed [26].

The SEM analysis (Fig. 8a–d) is carried out on the outer surface which wear-out at constant speed of 75 rpm and for different loads of 33, 45 and 57 N to study the effect of load on the wear mechanisms. The outer surface (Fig. 8a) worn at low load (33 N) reveals very less quantity of material removal and this owes to the trouble-free rolling action of the abrasive particles between the specimen and the counter face without any effort at low load. On increasing the load (45 N) on this outer surface (Fig. 8b), the abrasive particles get compacted when moving between the surfaces due to increase in the contact pressure. This inturn causes the abrasive particles to damage mutually the rubber wheel and the specimen surface. Therefore, this surface reveals the ploughing action of the abrasive particles on the composite surface. Turning to high load (57 N) on this surface (Fig. 8c), more cutting and ploughing action on the specimen surface is observed which leads to more material removal. The unreinforced aluminium alloy (Fig. 8d) subjected to high load (57 N) at the speed of 75 rpm reveals deeper grooves and more amount of deformation on the surface. This is due to easy abrading action of the abrasive particles on the softer matrix surface.

8.4.2 Effect of Speed on Abrasion Wear Rate

The FGAMMC is tested for its abrasive wear behaviour under different speed of 75, 125 and 175 rpm on outer, middle and inner surface at different distance of 1, 7 and 13 mm from the outer periphery of the casting and on unreinforced alloy surface are shown in Fig. 9a–c. The wear test is conducted at constant loads of 33, 45 and 57 N to learn the effect of speed on wear rate of the composite specimens. From Fig. 9a–c, it is observed that, wear rate increases linearly with speed at all the load conditions and on all the surfaces at different distance from the outer periphery of the casting. The wear rate is maximum at high speed and may be due to the increase in frequency of

contact of the counter face with the specimen surfaces, which produces more material removal. This may also be due to the fact that the abrasive medium at high speed uses more of its energy in eroding the specimen and result in more material removal. It is observed from the Fig. 9a–c, the outer, middle and inner surfaces at different distance of FGM shows less wear rate than the unreinforced alloy on all speed conditions at constant load, where the similar trend is observed [27].

To study the effect of speed on the wear transition, inner surface worn at different speed (75, 125 and 175 rpm) and at constant load (45 N) is taken for SEM analysis (Fig. 10a–d). This inner surface usually has more matrix area and therefore it reveals more material removal at all the speed conditions but less worn than the aluminium alloy. At low speed of 75 rpm and load of 45 N, the
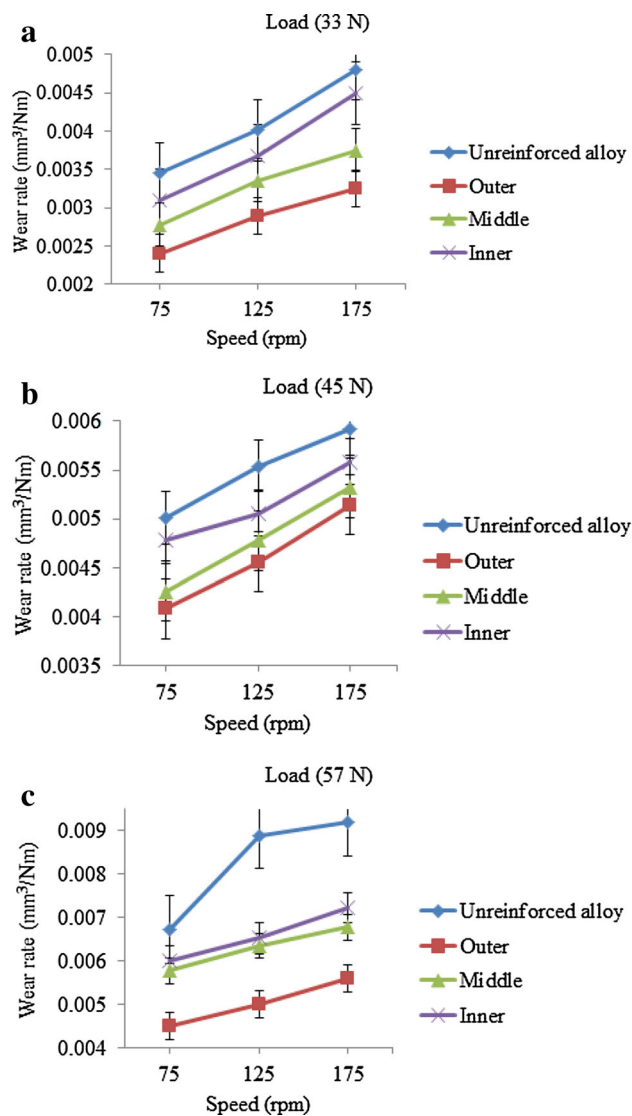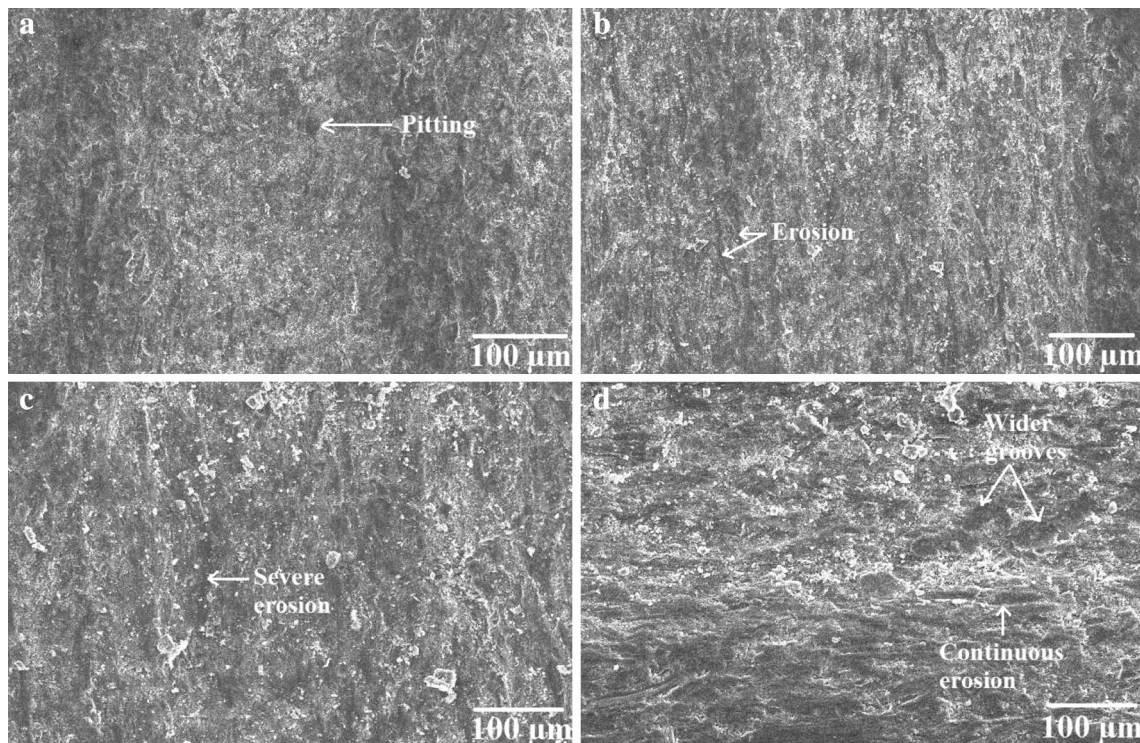

Fig. 9 a–c Effect of speed on wear rate

Fig. 10 SEM analysis of inner surface of FGM at **a** 75 rpm **b** 125 rpm **c** 175 rpm and **d** Unreinforced alloy (175 rpm)

abrasive particles are incapable to gain energy from the slow rotating wheel to produce erosion on the specimen surface. Therefore, this surface (Fig. 10a) reveals only tiny amount of erosion behaviour with less number of pitting. As the speed increases to 125 rpm on the inner surface (Fig. 10b), the surface is pitted and grooved by abrasive particles which gets more energy from the fast rotating rubber wheel. The eroding action of the abrasive particles get severe when the speed is raised to high level of 175 rpm and the surface (Fig. 10c) shows the removal of more material and the same behaviour is observed [28]. The unreinforced alloy (Fig. 10d), worn at the speed of 175 rpm and at load of 45 N reveals severe cutting and wider grooves along with debris formation. This is because of the sharp silica sand abrasive medium which is harder than the matrix surface and produces continuous erosion on the matrix surface leading to maximum material removal.

8.4.3 Effect of Distance and Alloy on Abrasion Wear Rate

The effect of different distance from the outer periphery of the casting on the abrasion wear rate is studied and shown in Fig. 11a–f. The FGAMMC is tested for constant load (Fig. 11a–c) and constant speed (Fig. 11d–f) individually. The plots reveal that the abrasion wear rate increases with increase in distance from the outer periphery of the casting for all load and speed condition. The outer surface at the

distance of 1 mm tested at different load (Fig. 11a–c) shows minimum wear rate when compared to the surfaces at the distances of 7 and 13 mm respectively. This might be due to the fact that the surface at the distance of 1 mm from outer periphery has more reinforcement particles and protects the surface from wear rate. The surface at a distance of 1 mm has contact of the reinforcement particles only with the counter face thereby reducing the real contact area of the aluminium matrix with the rubber wheel. This inturn bears the load and avoids transmitting the load to the matrix alloy, and results in less wear compared to the middle and inner surface at all load. The reinforcement particles usually have the higher hardness when compared to the matrix alloy and protects the matrix from wear at all load. The hardness of this surface protects the material from severe ploughing, indentation and abrasion effects of the abrasive medium on the specimen surface and consequences in less wear rate.

On the other hand, the middle and inner surfaces at the distance of 7 and 13 mm from the outer periphery of the casting which has less reinforcement particles experiences severe indentation and ploughing, which leads to more material removal. This shows eventually that the outer surface at a distance of 1 mm has higher hardness (145 HV) compared to the middle and inner surface at distances of 7 mm (130 HV) and 13 mm (105 HV) from the outer periphery of the casting. The unreinforced alloy
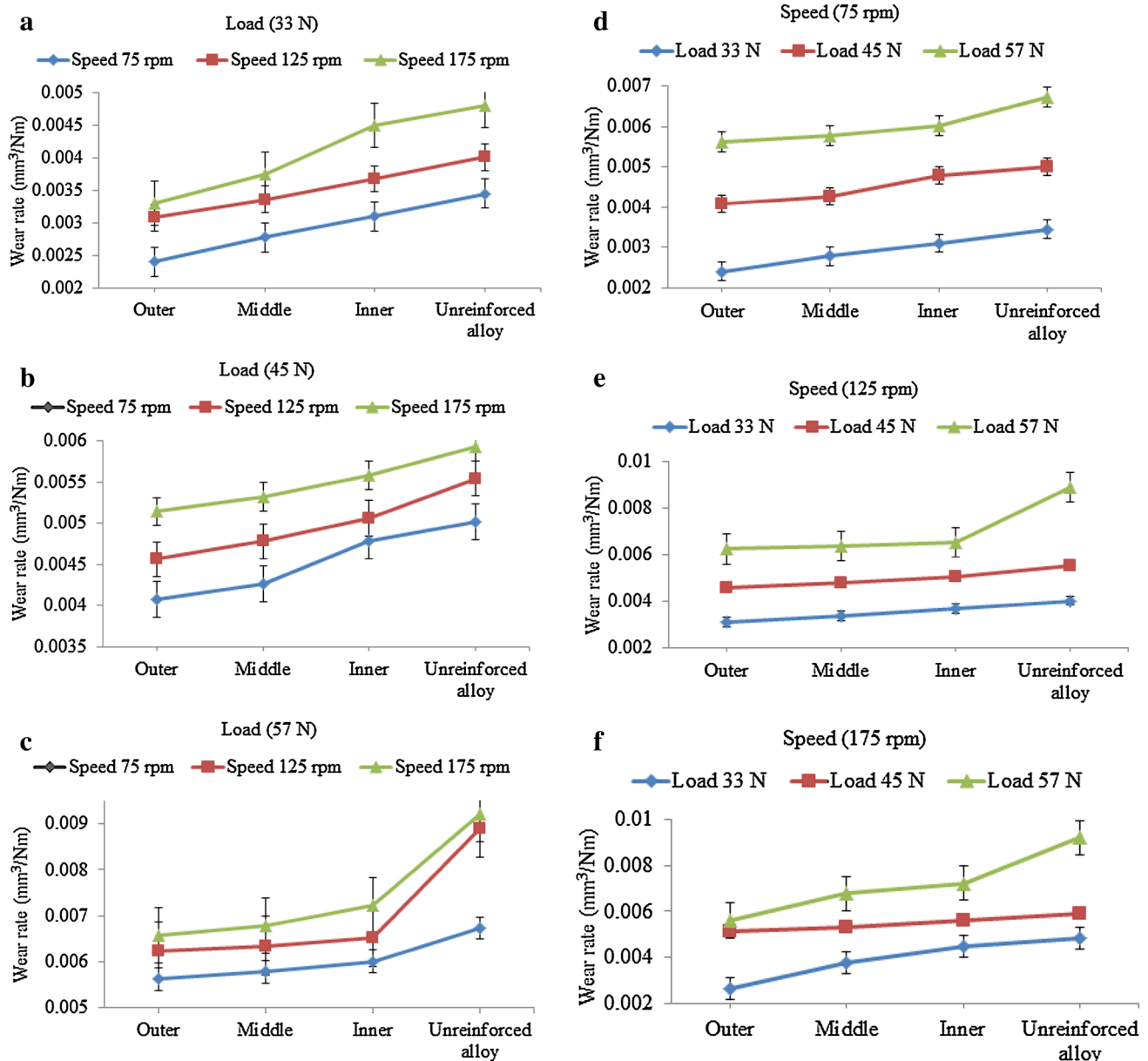
Fig. 11 **a–f** Effect of distance and alloy on wear rate

has the least hardness of 87 HV and subjected to high abrasion rate on all the test conditions which shows that hardness is directly associated to the wear resistance. Therefore, it is observed that particle enriched area has higher wear resistance and the particle depleted area has lesser wear resistance, where the analogous behaviour is observed [29]. As like the trend observed for wear rate for different distances from the outer periphery corresponding to constant load of 33, 45 and 57 N, same behaviour of wear rate is observed with respect to constant speed of 75, 125 and 175 rpm.

The surface of unreinforced alloy and the outer, middle and inner surfaces of FGM worn at high load (57 N) and

high speed (175 rpm) are taken for SEM analysis (Fig. 12a–d). The outer surface (Fig. 12a), subjected to high load and high speed reveals the cutting on the surface with less material removal due to the presence of more reinforcement particles on the surface. This surface resists the ploughing action at high load and eroding action of abrasive particles at high speed due to the better hardness of the highly reinforced region. The middle surface (Fig. 12b), worn at same condition reveals grooving on the surface with more material removal than the outer surface due to less hardness of the surface. The inner surface (Fig. 12c), with less reinforcement particles reveals more indentation caused by the abrasive particles at high speed
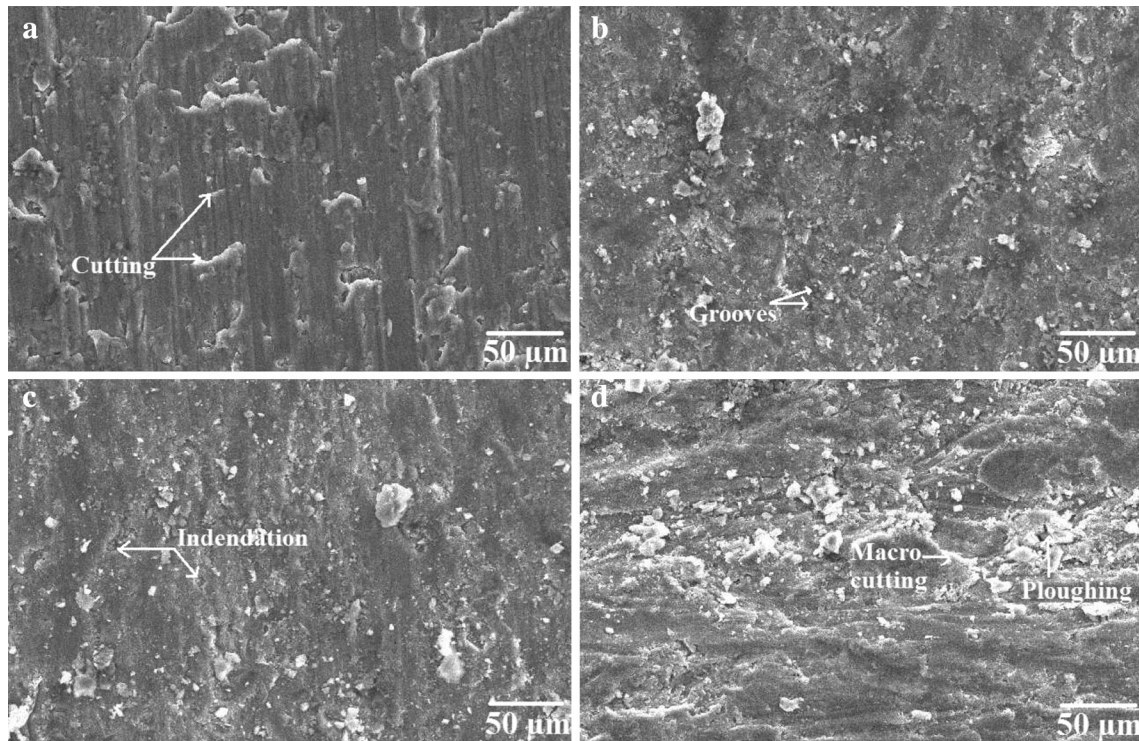
Fig. 12 a–d SEM analysis of FGM at **a** Outer surface **b** Middle surface **c** Inner surface and **d** Unreinforced alloy

and high load due to weaker matrix area with very less amount of reinforcement particles. The unreinforced alloy (Fig. 12d), suffers from macro cutting and ploughing along with continuous deep grooves due to its inability to resist the damage caused by the abrasive particles. This surface also reveals depth and extent of grooves due to the action of the abrasive particles which embeds on the rubber wheel.

9 Conclusion

Functionally graded Al-Si12Cu metal matrix composite with gradual distribution of reinforcement particles across the thickness of the casting is successfully achieved through centrifugal casting. The optical micrograph reveals the presence of more reinforcement particles on the outer surface at a distance of 1 mm and less reinforcement particles on the middle and inner surface at distances of 7 and 13 mm respectively. The tensile strength is more at the particle enriched zone and less at the particle depleted zone. The fractural analysis reveals that outer region of FGM fractures in a combined brittle-ductile manner. The hardness linearly decreases with increase in distance from the outer periphery of FGM and higher than the unreinforced alloy. The abrasion results reveal that higher the load, speed and distance from the outer periphery; higher

the wear rate. The worn surfaces reveal that all the surfaces of the FGM are with less material removal than the surface of the unreinforced aluminium alloy. In particular the outer surface of the FGM outperforms with high wear resistance than other surfaces. Thus functionally graded material developed with higher wear resistance at the outer surface can be utilized for overcoming the wear problems in automotive applications like brake drums and cylinder liners.

References

1. Uyyuru R K, Surappa M K, and Brusethaug S, *Tribol Int* **40** (2007) 365.
2. Christy T V, Murugan N, and Kumar S, *J Miner Mater Charact Eng* **9**(1) (2010) 57.
3. Singh L, Ram B, and Singh A, *Int J Res Eng Technol* **2**(8) (2013) 375.
4. Gopi K R, Mohandas K N, Reddappa H N, and Ramesh M R, *Int J Eng Adv Technol* **2**(5) (2013) 340.
5. Lozano D E, Mercado-Solis R D, Perez A J, Talamantes J, Morales F, and Hernandez Rodriguez M A L, *Wear* **267** (2009) 545.
6. Mishra AK, Sheokand R, and Srivastava R K, *Int J Sci Res Publ* **2**(10) (2012) 1.

7. Uthayakumar M, Aravindan S, and Rajkumar K, *Mater Des* **47** (2013) 456.

8. Zhang J, Wang Y-Q, Zhou B-L, and Wu X-Q, *J Mater Sci Lett* **17**, (1998) 1677.

9. Chen W, Wang Q, Zai C, Ma C, Zhu Y, and He W, *J Mater Sci Lett* **20** (2001) 823.

10. Gomes J R, Ramalho A, Gaspar M C, and Carvalho S F, *Wear* **259** (2005) 545.

11. Put S, Vleugels J, and Van der Biest O, *J Mater Process Technol* **143-144** (2003) 572.

12. Song C-J, Xu Z-M, and Li J-G, *Compos Part A* **38** (2007) 427.

13. Duque N B, Melgarejo Z H, and Suarez O M, *Mater Charact* **55** (2005) 167.

14. Derakhshesh M, Sina, H and Nazemi H, *Majlesi J Mech Eng* **4** (2011) 27.

15. Shivaji V. Gawali, and Vinod B. Tungikar, *Sastech J* **12** (2013) 15.

16. Rodriguez-Castro R, Wetherhold R C, Kelestemur M H, *Mater Sci Eng* **A323** (2002) 445.

17. Leon-Patinon C A, Aguilar-Reyes E A, Bedolla-Becerril E, Bedolla-Jacuinde A, and Mendez-Diaz S, *Wear* **301** (2013) 688.

18. Su B, Yan H G, Chen J H, Zeng P L, Chen G, and Chen C C, *J Mater Eng Perform* **22** (2013) 1355.

19. Humberto Melgarejo Z, Marcelo Suarez O, Sridharan, K (2008) Compos Part A 39 1150.

20. Vieira A C, Sequeira P D, Gomes J R, and Rocha L A, *Wear* **267** (2009) 585.

21. Barekar N, Tzamtzis S, Dhindaw B K, Patel J, Hari Babu N, and Fan Z, *J Mater Eng Perform* (2009).

22. Liu Q, Ke L, Liu F, Huang C, and Xing L, *Mater Des* **45** (2013) 343.

23. Lin C Y, Bathias C, Mc Shane H B, and Rawlings R D, *Powder Metall.* **42** (1999) 29.

24. Askari E, Mehrali M, Metselaar I H S C, Kadri N A, and Rahman Md M, *J Mech Behav Biomed Mater* **12** (2012) 144.

25. Radhika N, and Raghu R, *J Tribol* **137**(3) (2015) 1.

26. Kok M, and Ozdin K, *J Mater Process Technol* **183** (2007) 301.

27. Kumar S, and Balasubramanian V, *Tribol Int* **43** (2010) 414.

28. Agarwal G, Patnaik A, and Sharma R K, *Int J Eng Res Appl* **2** (2012) 1148.

29. Rajan T P D, Jayakumar E, and Pai B C, *Trans Indian Inst Met* **65** (6) (2012) 531.